New Unsymmetrical Bolaamphiphiles: Synthesis, Assembly with DNA, and Application for Gene Delivery

Namrata Jain, Youri Arntz, Valérie Goldschmidt, Guy Duportail, Yves Mély, and Andrey S. Klymchenko*

Laboratoire de Biophotonique et Pharmacologie, UMR 7213 CNRS, Université de Strasbourg, Faculté de Pharmacie, 74, Route du Rhin, 67401 ILLKIRCH Cedex, France. Received July 23, 2010; Revised Manuscript Received September 20, 2010

The success in gene therapy relies strongly on new efficient gene delivery vectors. Nonviral vectors based on lipids and polymers constitute an important alternative to the viral vectors. However, the key problem with these vectors is the poor structural control of their DNA complexes. In the present work, following new design we synthesized unsymmetrical bolaamphiphiles, molecules bearing neutral sugar (gluconic acid) and dicationic ornithine head groups connected by different long hydrophobic spacers. Within this design, a positively charged headgroup is expected to bind DNA, the hydrophobic spacer is to drive the formation of a monolayer membrane shell around DNA, while the neutral group is to be exposed outside of the complex. Our fluorescence and gel electrophoresis data showed that self-assembly of bolas and their interaction with DNA depend strongly on the bola structure. The size of bola/DNA complexes (bolaplexes) estimated from dynamic light scattering data was ~100 nm at low N/P (cationic nitrogen/DNA phosphate molar ratio), while at higher N/Ps it was significantly larger due to neutralization of their surface charge. Atomic force microscopy studies revealed nanostructural rod-shaped or spherical morphology of the bolaplexes. Transfection efficiency of the bolaplexes in vitro was significant when either DOPE or chloroquine were used as helping agents, suggesting that the key barrier for their internalization is the endosomal escape. Finally, all bolas showed low cytotoxicity (cell viability >80%). The present results show that bolas are prospective candidates for construction of nonviral gene delivery vectors. We believe that further optimization of polar head groups and a hydrophobic spacer in the bolas will lead to vectors with controlled small size and high transfection efficiency.

INTRODUCTION

The vast majority of natural and synthetic lipids studied so far are "monopolar" amphiphiles, that is, molecules presenting one polar headgroup and generally two hydrophobic chains. However, bipolar amphiphiles, which are analogues of lipids presenting polar groups at the two opposite sides of the hydrophobic chain(s), so-called bolaamphiphiles (bolas), became the matter of intensive research only in the recent years (*1*). A remarkable feature of bolas is that in contrast to bilayer membranes formed by lipids they can form monolayer membranes (Figure 1), having bolas with membrane-spanning hydrophobic chains, which are believed to be responsible for enhanced physical stability of bola membranes (*1, 2*). In nature, they are mainly present in archaebacteria and ensure the integrity of the bacterial membrane at high temperature (90 °C) and low pH (1−1.5) (*3, 4*). Membranes made from synthetic bolas, forming either nanotubes or vesicles, can also show an exceptional stability, some of them being stable even in the dry phase (*5, 6*) or in some organic solvents (*7*). Unsymmetrical bolas, bearing two different polar head groups, assembled in a parallel fashion can form asymmetric membranes, so that the two opposite sides of the monolayer membrane present different functional groups (Figure 1) (*5, 6*). One of the attractive applications of bolas, which is still in its infancy stage, is gene delivery, a domain for which "monopolar" cationic lipids and other cationic agents are currently maintaining a dominant position.

Gene delivery, which is a main concern in gene therapy, relies heavily on development of new delivery vectors. Nonviral vectors based on lipids are highly attractive, since they can deliver large quantities of genetic information and are weakly immunogenic (*8*). A variety of cationic lipids for gene delivery has been developed in recent decades (*8*−*19*). Their complexes with DNA (lipoplexes) show high transfection efficiency in vitro, though their application for gene therapy in vivo remains a challenge. One of the key problems of cationic lipids is the poor structural control of their lipoplexes (*10, 20*). Indeed, symmetric lipid bilayers made of cationic lipids interact with DNA by forming infinite sandwich-like structures of high polydispersity (Figure 1) (*10*).

In this respect, unsymmetrical bolas bearing positively charged and neutral head groups could be an attractive alternative to the cationic lipids. These molecules could generate asymmetric membranes (in form of vesicles or nanotubes) having positively charged inner and neutral outer surfaces. In such a case, the inner membrane surface can be used to wrap the DNA molecule (Figure 1), while the outer neutral membrane surface, being inert to DNA, would prevent further oligomerization of the complex and could be utilized for efficient exposure of the biological signal for specific targeting. The examples of successful application of bolas for gene delivery, which has been shown only in the recent years, include synthetic unsymmetrical bolas (*21*−*25*) and archaebacteria-derived lipids (*26, 27*). Among unsymmetrical bolas, the most promising were those bearing a sugar (gluconic or lactonic acid) residue on one side and mono- or oligo-cationic ammonium-based group on the other (*21, 23*). Moreover, the galactose-bearing bolas showed some specificity to HepG2 cell line, expressing a galactose receptor of endocytosis (*21, 22*).

In the present work, three new bolaamphiphiles were synthesized, bearing neutral sugar and dicationic ornithine head groups, connected by different hydrophobic spacers. We showed

* To whom correspondence should be addressed. E-mail: andrey.klymchenko@unistra.fr. Fax: +33 368 854313. Tel: +33 368 854255.

10.1021/bc100334t © 2010 American Chemical Society
Published on Web 10/14/2010

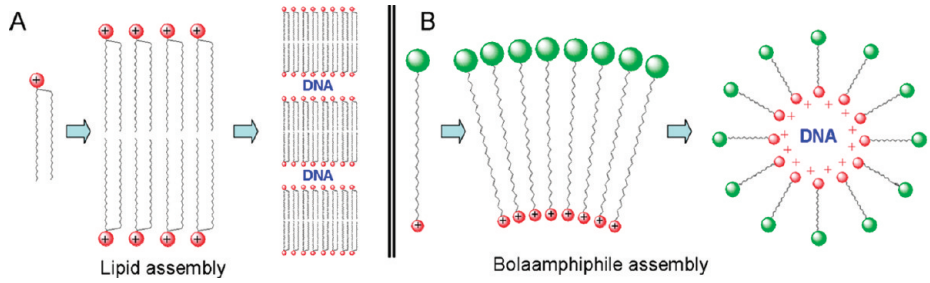

Figure 1. Lipids and bolaamphiphiles assembly with DNA. (A) Schematic presentation of bilayers formed from cationic lipids and further formation of DNA complexes, so-called lipoplexes. (B) Assembly of bolaamphiphiles into asymmetric membranes and formation of DNA complexes, so-called bolaplexes.

that the nature of spacer defines the bola self-assembly, the interaction with DNA and the morphology of the obtained complexes. Moreover, some bolas can transfect efficiently COS-7 cells in the presence of either a helper lipid (DOPE) or an endosomolytic reagent (chloroquine) (*28*). The latter indicates that the key barrier for gene delivery with the present bolas resides in the endosomal escape. This work presents new bolaamphiphile-based nonviral vectors and provides insights for further improvements of their efficiency.

MATERIALS AND METHODS

All chemicals and solvents for synthesis were purchased from Sigma-Aldrich. Mass spectra were measured using Mass Spectrometer Mariner System 5155. LC-MASS was performed on Agilent, 1956 B/MSD. ^{1}H NMR spectra were recorded on Bruker 300 MHz spectrometer.

***N*-Boc-4-aminophenol (1).** 4-Aminophenol (4 g, 36.7 mmol) and Boc_2O (8 g, 36.7 mmol) were dissolved in 30 mL of THF and left stirring overnight. Then 100 mL of water was added and the product was extracted with ethyl acetate (3 × 50 mL) and further dried with sodium sulfate. After solvent evaporation in vacuo, the crude product **1** was used without further purification.

16-(4-tert-Butoxycarbonylaminophenoxy)-hexadecanoic Acid Methyl Ester (2). Boc-protected 4-aminophenol (**1**) (1.8 g, 8.6 mmol) and 16-bromohexadecanoic acid methyl ester (3 g, 8.6 mmol, prepared by methylation of the acid in methanol and thionyl chloride) were dissolved in 10 mL of DMF and supplemented with 1.8 g (13 mmol) of potassium carbonate. After 12 h of stirring at room temperature (RT), the solution was poured in water (50 mL) and the product was extracted with dichloromethane (3 × 30 mL) and dried with sodium sulfate. Then the solvent was removed and the product **2** (1.6 g, 40%) was crystallized from ethanol. ^{1}H NMR ($CDCl_3$, 300 MHz): δ 7.24 (d, 2H), 6.82 (d, 2H), 6.4 (s, 1H), 3.91 (t, 2H), 3.67 (s, 3H), 2.31 (t, 2H), 1.82−1.58 (m, 4H), 1.55−1.48 (m, 9H), 1.46−1.2 (m, 24H). LC-MS (*m*/*z*): found $[M + 1]^+$ = 378.2; calcd for $C_{28}H_{47}NO_5^+$-$C_5H_9O_2$ (Boc) = 378.3.

16-[4-(2,5-Bis-tert-butoxycaronylamino-pentanoylamino)-phenoxy]-hexadecanoic Acid Methyl Ester (3). Boc was removed from **2** (3.14 mmol, 1.5 g) by treating with 5 mL TFA and 3% H_2O for 1 h at RT. The solvent was evaporated and 1.54 g (3.1 mmol) of the obtained deprotected amine was coupled with 2,5-bis-tert-butoxycarbonyl amino-pentanoic acid (3.57 mmol, 1.15 g) using BOP (3.44 mmol, 1.52 g), HOBt (4.3 mmol, 0.58 g), and DIEA (12.6 mmol, 2.2 mL) in DMF (15 mL) and dichloromethane (30 mL). The mixture was stirred overnight at RT. Then, solvent was evaporated and product was crystallized from acetonitrile. The precipitate was filtered off and dried to give compound **3** (1.6 g, 76%). ^{1}H NMR ($CDCl_3$, 300 MHz): δ 8.41 (s, 1H), 7.41 (d, 2H), 6.81 (d, 2H), 5.25 (s, 1H), 4.73 (s, 1H), 4.39 (s, 1H), 3.9 (t, 2H), 3.65 (s, 3H), 3.4 (s, 1H), 3.09 (s, 1H), 2.28 (t, 2H), 1.83−1.69 (m, 4H), 1.67−1.53 (m, 4H), 1.47−1.38 (m, 18H), 1.37−1.16 (m, 22H). LC-MS (*m*/*z*): found $[M + 1]^+$ = 491.2; calcd for $C_{38}H_{65}N_3O_8^+$-$C_{10}H_{18}O_4$ (2Boc) = 491.2.

(1-{4-[15-(2-Amino-ethylcarbamoyl)-pentadecyloxy]-phenylcarbamoyl}-4-tert-butoxycabonylamino-butyl)-carbamic Acid tert-Butyl Ester (4). Methyl ester of **3** (0.7 mmol, 0.5 g) was substituted with ethylenediamine (150 mmol, 10 mL) for 72 h at 70 °C. Then the excess of ethylenediamine was evaporated, 50 mL of water was added and the product **4** was filtered (0.45 g, 87%). ^{1}H NMR ($CDCl_3$, 300 MHz): δ 8.45 (s, 1H), 7.42 (d, 2H), 6.82 (d, 2H), 6.05 (s, 1H), 5.30 (s, 1H), 4.75 (s, 1H), 4.37 (s, 1H), 3.91 (t, 2H), 3.42−3.25 (m, 3H), 3.16−3.02 (m, 1H), 2.84 (t, 2H), 2.17 (t, 2H), 2.06−1.92 (m, 4H), 1.79−1.7 (m, 2H), 1.67−1.54 (m, 4H), 1.48−1.37 (m, 18H), 1.37−1.20 (m, 20H). LC-MS (*m*/*z*): found $[M + 1]^+$ = 720.4; calcd for $C_{39}H_{69}N_5O_7^+$ = 720.4.

[4-tert-Butoxylamino-4-(4-{15-[2-(2,3,4,5,6-pentahydroxy-hexanoylamino)-ethylcabamoyl]-pentadecyloxy}-phenylcarbamoyl)-butyl]-carbamic Acid tert-Butyl Ester (5). D-gluconic acid δ-lactone (0.23 mmol, 0.04 g) was added to solution of **4** (0.11 mmol, 0.1 g) in 15 mL of methanol. Then, DIEA (1.4 mmol, 0.24 mL) was added and the reaction mixture was stirred at 70 °C for about 24 h. Solvents were evaporated in vacuo. Compound **5** (0.09 g, 90%) was crystallized from methanol. ^{1}H NMR (CD_3OD, 300 MHz): δ 7.42 (d, 2H), 6.87 (d, 2H), 4.21 (s, 1H), 4.18−4.06 (m, 2H), 3.96 (t, 2H), 3.83−3.6 (m, 5H), 3.09 (t, 2H), 2.19 (t, 2H), 1.86−1.54 (m, 10H), 1.48−1.41 (m, 18H), 1.39−1.26 (m, 22H). LC-MS (*m*/*z*): found $[M + 1]^+$ = 898.57; calcd for $C_{45}H_{79}N_5O_{13}^+$ = 898.57.

16-[4-(2,5-Diamino-pentanoylamino)-phenoxy]-hexadecanoica-cid[2-(2,3,4,5,6-pentahydroxy-hexanoylamino)-ethyl]-amide (Orn-C16-G). Boc was removed from 50 mg of **5** using 0.5 mL TFA and 3% H_2O (1 h) to get the final product Orn-C16-G (27 mg, 90%). LC-MS (Bruker, HTCultra) (*m*/*z*): found $[M + 1]^+$ = 698.4; calcd for $C_{35}H_{64}N_5O_9^+$ = 698.4.

Fluorescence Measurements. Absorption spectra were recorded on a Cary 400 spectrophotometer (Varian) and fluorescence spectra either on FluoroMax 3.0 or Fluorolog (Jobin Yvon, Horiba) spectrofluorimeters. All the emission spectra were corrected from the background signal of the corresponding blank (corresponding solution without the fluorescent dye). For measurements with 1,8-ANS, 50 nM of the dye dissolved in 20 mM MES buffer (pH 7.4 or 6.0) solution was titrated with increasing quantities of the corresponding bola, added from stock solutions. All spectra were recorded 2 min after each addition. In the ethidium bromide (EtBr) exclusion assay, an aliquot of CT-DNA (final concentration 20 μM) was added to the solution of EtBr (0.4 μM). After 2 min, increasing quantities of the corresponding bola were added from stock solutions (in DMF with 10% of water). Fluorescence intensity recorded at 600 nm (excitation at 550 nm) was recorded 2 min after each addition of bola aliquot.

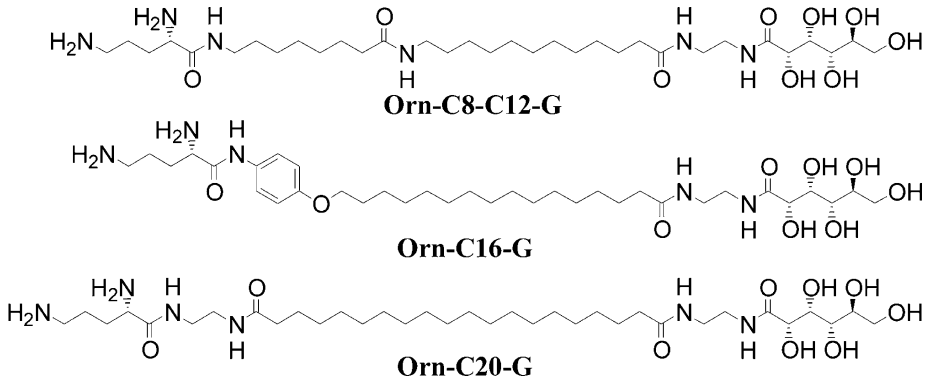

Figure 2. Chemical structures of bolaamphiphiles.

Dynamic Light Scattering (DLS) and ζ-Potential Measurements. The bolaplexes were prepared in 20 mM MES at pH 7.4 by mixing equal volumes of the solutions of calf thymus DNA (CT-DNA) or pCMV-Luc plasmid (pDNA) and the corresponding bolas. The bola solutions were prepared by adding aliquots of their stock solutions (in DMF with 10% of water) to the buffer. The final DNA concentration (expressed in phosphate) was 20 μM, while the bolas concentration was adjusted according to a desired N/P ratio. The N/P ratio between bolas and pDNA was expressed as the molar ratio between all the protonable amino groups of the bolas and the phosphate groups of the DNA. The DLS measurements were performed after 30 min of incubation at room temperature. The average size of the complexes was determined with a Zetasizer Nano ZS (Malvern Instruments) with the following specifications: sampling time, 30 s; medium viscosity, 0.8872 cP; refractive index (RI) medium, 1.33; RI particle, 1.590; scattering angle, 90°; temperature, 25 °C. For particle analysis, the statistics based on particle volume and particle number were presented. For ζ-potential measurements, the same sample preparation was done using CT-DNA at 30 μM concentration. The instrumental specifications were the same, accounting for a solvent dielectric constant of 78.5.

Gel Electrophoresis. The bolaplexes were prepared at different N/P ratios using 60 μM pCMV-Luc plasmid (final phosphate concentration), followed by 30 min incubation at room temperature. Four microliters of loading dye (Lonza, 6×) was added to 20 μL of the prepared complexes and then 12 μL of this mixture was loaded on 0.9% agarose gel prepared with 0.5X TAE (tris-acetate-ethylenediaminetetraacetic acid) buffer. In parallel, a 10 kbp DNA ladder (Lonza) was loaded on the gel. Electrophoresis was carried out with 0.5X TAE buffer at a constant voltage of 100 mV. DNA bands were visualized by UV trans-illuminator (GeneGenius, Syngene) after coloration with EtBr (0.5 μg/mL) for 15 min.

AFM Measurements. AFM measurements were performed using the Solver Pro-M (NT-MDT) instrument. The measurements were performed in liquid phase (MES buffer pH 7.4) by using the tapping mode. The cantilevers used were NSG03 type (NT-MDT) with a typical spring constant of 1.7 N/m, a resonance frequency of 32 kHz in liquid, and a tip curvature radius of 10 nm. Images were acquired with a resolution of 512 × 512 and a scan rate of 2 Hz. The samples were prepared as for DLS measurements, then 100 μL of the solution was deposited on the freshly cleaved mica followed by the addition of 10 μL of a $MgCl_2$ stock solution to obtain a final concentration of 10 mM. The measurements were performed 10 min after sample preparation.

Transfection and Cytotoxicity. COS-7 cells (African Green Monkey kidney fibroblast cell line) were grown in Dulbecco's modified Eagle's medium (Gibco-Intvitogen), supplemented with 10% fetal bovine serum (FBS, Lonza) and 100 U/ml of penicillin and streptomycin (Gibco-Intvitogen) at 37 °C in a humidified atmosphere containing 5% CO_2. Cells were seeded at a density of 1×10^5 cells in a 24-well plate, 24 h before transfection.

Transfection was done by using bola/pDNA (pCMV-Luc plasmid, 1 μg/well) complexes at different N/P ratios in serum-free Opti-MEM (Gibco-Invitrogen) or complete culture medium (DMEM containing 10% of FBS). For this purpose, bolaplexes were prepared in MES buffer (pH 7.4) as for DLS measurements and then added to the cells in Opti-MEM. Chloroquine (100 μM) or DOPE (1:1 molar ratio with respect to bola) was used to enhance transfection efficiency in some formulations. In formulations with DOPE, a mixture of DOPE and a corresponding bola in ethanol was evaporated in a round-bottom flask to obtain a film. Then, MES buffer (pH 7.4) was added and the samples were hydrated overnight at RT. Then, the samples were vortexed vigorously for 1 min and further sonicated in an ultrasonic bath for 15 min. The obtained suspensions were mixed with an equal volume of pDNA in the buffer to obtain a desired N/P ratio. All formulations were incubated at RT for 30 min before addition to the cells. After 3 h of incubation of cells with bolaplexes at 37 °C, 10% of FBS was added to serum-free samples, while for all the samples with chloroquine the transfection medium was replaced with fresh complete culture medium and then cells were cultured for another 45 h. Total incubation time for all samples was 48 h. Luciferase gene expression of lysed cells was quantified using a commercial kit (Invitrogen) and a luminometer (CentroXS^3 LB 960, BERTHOLD Technologies). Results were expressed as relative light units integrated over 10 s per mg of total cell protein lysate (RLU/mg of total protein). The experiments were repeated six times for serum-free samples and three times for samples with serum. The total protein was determined by BC assay (Protein Quantitation Kit, Interchim) using Cary 4000 spectrophotometer. As a positive control in the transfection measurements, commercially available agent jetPEI (Polyplus) was used following protocols provided in the kit.

Cytotoxicity of bolas was evaluated using 3-(4,5-dimethyl-2-thiazolyl)-2,5-diphenyltetrazolium bromide (MTT, Sigma-Aldrich) assay (*29*). COS-7 cells were seeded in a 24-well plate at 1×10^5 cells per well and after 24 h of incubation at 37 °C supplemented with bolas at different concentrations or jetPEI (150 μM, expressed as concentration of nitrogen residues) in serum-free Opti-MEM. After incubation for 3 h at 37 °C, 10% of FBS was added and cells were cultured for another 45 h. Cells were washed with phosphate buffer saline (PBS) and incubated with serum free medium containing 0.5 mg/mL MTT for 3 h at 37 °C. Media was discarded and formazan crystals were resuspended in 0.5 mL MTT solvent (Sigma-Aldrich). Absorbance of formazan solution was measured at 570 nm with

Scheme 1. Synthesis of Bola Orn-C16-G

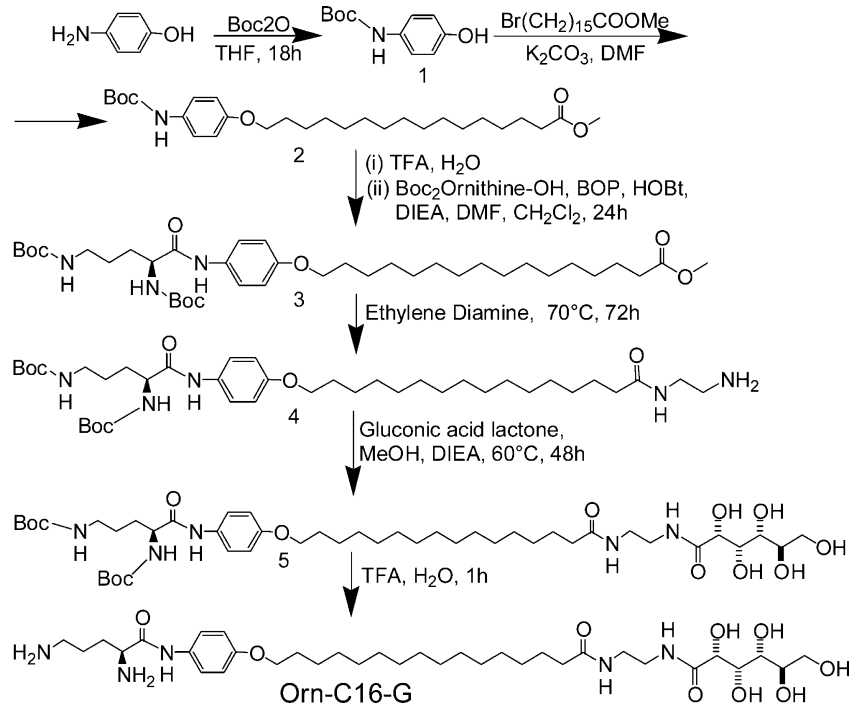

respect to the background at 690 nm using Cary 4000 spectrophotometer. Cell viability was expressed as relative absorbance (%) of the sample versus control cells.

RESULTS AND DISCUSSION

Design and Synthesis. The basic design of bolas relies on one neutral group and one dicationic group connected by a hydrophobic spacer. As neutral group we selected a sugar residue, which is biocompatible and relatively inert. The dicationic headgroup responsible for DNA binding was the ornithine residue (Orn), featuring two amino groups separated by a 4-carbon atom distance. This distance ensures protonation of both amino groups at neutral pH and thereby efficient interaction with negatively charged DNA. On the basis of this design, three new bolaamphiphiles were synthesized, presenting different hydrophobic spacers: (a) a dipeptide composed of end-substituted amino acids of 8- and 12-carbon atoms, Orn-C8-C12-G; (b) a hydrophobic linker composed of an alkyl chain of C16-carbon atoms and an aromatic unit, Orn-C16-G; and (c) a long (20-carbon atoms) alkyl chain, Orn-C20-G (Figure 2). This variation of the hydrophobic spacer could tune the hydrophobic, H-bonding and π-stacking interactions between bolas. An example of synthesis of Orn-C16-G is presented in Scheme 1. Initially, the amino group of 4-aminophenol was protected with Boc-group (**1**) and its hydroxyl was further reacted with methyl 16-bromohexadecanoate. Then, the amino group in the obtained conjugate **2** was further deprotected and substituted with Boc-protected ornithine. The obtained conjugate **3** was further reacted with ethylene diamine giving **4**. The latter was then substituted with D-gluconic acid δ-lactone followed by Boc-removal, affording final bola Orn-C16-G. The yields of the individual steps were systematically >50% and the obtained final bolas in 100−200 mg quantities were sufficiently pure according to NMR, LC-MS and HPLC techniques (see also Supporting Information).

Self-Assembly. 1,8-ANS dye is poorly fluorescent in water, while on binding to lipid membranes it becomes strongly fluorescent (*30*). In the present work, we used this probe to study the concentration-dependent bolas assembly. Solutions at pH 7.4 and 6.0 were tested, which could alter the protonation of the amino groups of bolas in the self-assembled state. It can be seen from Figure 3 that for Orn-C16-G at pH 7.4, fluorescence intensity grows rapidly with bola concentration showing beginning of saturation at higher concentrations. In contrast, at pH 6.0, a moderate increase in fluorescence intensity is followed by rapid increase at concentrations >20 μM. These data suggest that the critical aggregation concentration (CAC) at pH 7.4 is too low to be detected with this method, while at pH 6.0 it is clearly much larger being close to 20 μM. We could speculate that the self-assembly could be accompanied by a partial deprotonation of bola amino groups, so that lower pH may favor disassembly (i.e., higher CAC). In contrast, for bola Orn-C20-G rapid increase of 1,8-ANS fluorescence intensity was observed both at pH 7.4 (see Figure S1 in Supporting Information) and 6.0 (Figure 3). This indicates that CAC of Orn-C20-G is much

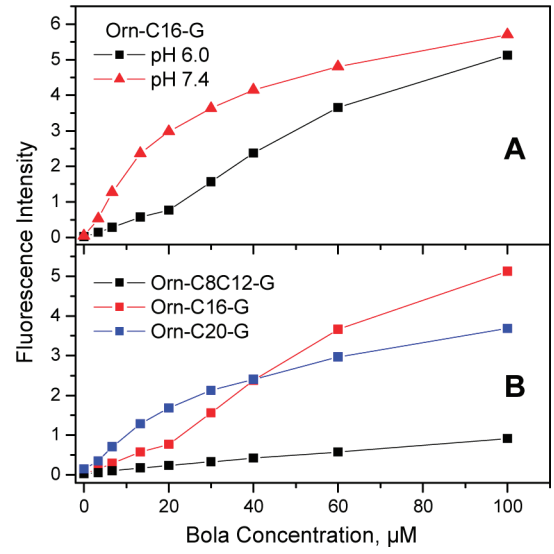

Figure 3. Fluorescence intensity of 1,8-ANS (50 nM) as a function of bolas concentration. (A) Orn-C16-G in MES buffer at pH 7.4 and 6. (B) Three different bolas at pH 6.

Table 1. Dynamic Light Scattering Data of Bolas and Bolaplexes in Aqueous Buffer (pH 7.4)

		volume analysis		
	sample	diameter, nm	amount, %	number analysis mean diameter, nm
Orn-C16-G	bola (100 μM)	110	88	73
		1450	12	
	bola/pDNA N/P 1.2 (12 μM bola)	109	95	90
	bola/pDNA	92	45	152
	N/P 2 (12 μM bola)	510	55	
	bola/pDNA N/P 2 (20 μM bola)	1550	95	1400
	bola/pDNA N/P 5 (50 μM bola)	870	100	925
	bola (100 μM)	140	15	110
		1050	85	
	bola/pDNA	97	20	90
	N/P 1.2 (12 μM bola)	930	80	
Orn-C20-G	bola/pDNA N/P 2 (12 μM bola)	970	100	900
	bola/pDNA N/P 2 (20 μM bola)	1370	100	1200
	bola/pDNA N/P 5 (50 μM bola)	1090	100	1069
	bola/DOPE (100 μM bola)	220	30	140
		1120	70	
Orn-C16-G/DOPE (1:1)	bola/DOPE/pDNA N/P 2 (20 μM bola)	220	100	218
	bola/DOPE/pDNA N/P 3 (30 μM bola)	200	20	190
		800	80	
	bola/DOPE/pDNA N/P 5 (50 μM bola)	1440	100	1350

lower than that of Orn-C16-G, probably because of its hydrophobic spacer, which is longer and does not contain bulky aromatic group, thus ensuring tight bola packing. Finally, Orn-C8-C12-G showed relatively weak increase in the fluorescence of 1,8-ANS with increasing concentration suggesting that it does not assemble at the studied concentration range. The latter result is probably connected to the presence of an amide group within the bola hydrophobic spacer, which may strongly diminish its hydrophobic interactions and thus increase its CAC.

The information about molecular order of bolas assemblies can be provided from fluorescence anisotropy of a rod-shaped molecule TMA-DPH (*31*). The observed values of fluorescence anisotropy for Orn-C16-G and Orn-C20-G assemblies at 100 μM are relatively high (0.30−0.32) at 20 °C and correspond to a rigid and highly ordered environment similar to lipid membranes in solid gel phase (0.32) for DPPC at 20 °C (data not shown) (*32*). These high values of fluorescence anisotropy suggest that bolas are probably organized in monolayers with a transmembrane spanning orientation, thus excluding possible bolas bilayer structure presenting a U-shaped conformation, as reported for some other bolas (*33*).

According to DLS data, Orn-C16-G and Orn-C20-G at 100 μM concentration form a significant fraction of small structures (around 100 nm, Table 1) in line with fluorescence data suggesting self-assembly of bolas at these conditions. These structures were stable for 1−2 h, while after longer incubation some precipitation of the bolas was observed.

Interactions with DNA. To study interactions of bolas with DNA, gel electrophoresis was first used. It can be seen from Figure 4A that Orn-C8-C12-G forms complexes with firefly luciferase plasmid DNA (pDNA) only at high N/P ratios (ratio between cationic groups of bola and phosphate groups of DNA). Indeed, only at N/P > 10 the pDNA band disappears. This indicates a relatively weak affinity of this bola to DNA. In contrast, Orn-C16-G (Figure 4B) and Orn-C20-G (Figure 4C) form complexes with pDNA at N/P values close to 1.0−1.2. It can be noted that Orn-C20-G shows a slightly stronger interaction since the DNA band disappears at lower N/P ratio (1.2) as compared to Orn-C16-G (1.6). By taking into account that all bola molecules are bearing the same dicationic ornithine residue, the stronger interaction of Orn-C16-G and Orn-C20-G with DNA is probably connected with a higher hydrophobicity of their spacers, which in turn favors their self-assembly and their cooperative interaction with DNA. Thus, we can assert that the interaction of the present bolas with DNA is controlled in part by their ability to self-assemble. Finally, a mixture of Orn-C16-G with a helper lipid DOPE (1:1 molar ratio with respect to bola), which was important in our transfection experiments (see below), showed complex formation at slightly higher N/P ratio, being completed at N/P 3 (see Figure S2 in Supporting Information).

The DNA condensation within the bolaplexes can be followed by the ethidium bromide (EtBr) exclusion assay (*34*). This dye when intercalated into DNA is highly fluorescent, while after DNA condensation it is expelled from its intercalation site, thus resulting in a strong decrease of its fluorescence intensity (up to 90%). For these studies, a linear DNA from calf thymus was used as the model. According to our data, Orn-C8-C12-G showed a relatively weak and rather linear decrease of EtBr fluorescence intensity as a function of N/P ratio (Figure 5), which is in line with the gel electrophoresis data showing its

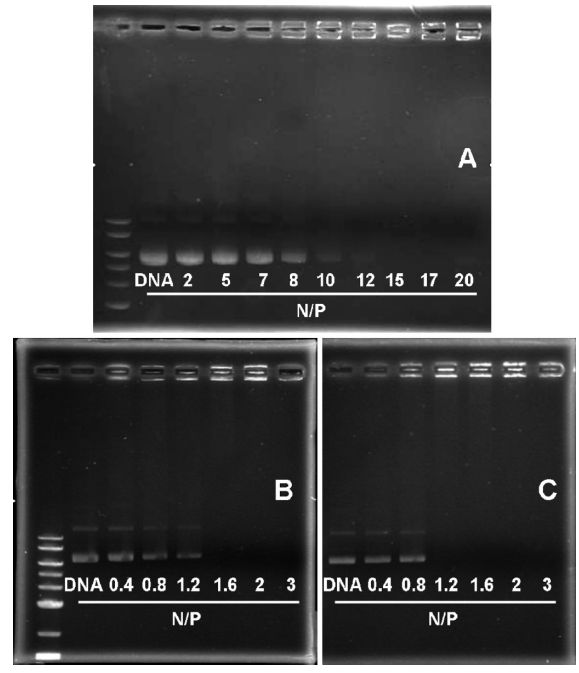

Figure 4. Agarose gel electrophoresis (0.9%) of Orn-C8-C12-G (A), Orn-C16-G (B), and Orn-C20-G (C) complexed with pDNA at different N/P ratios. Bands at the left of gels (A) and (B) correspond to 10 kbp DNA ladder.

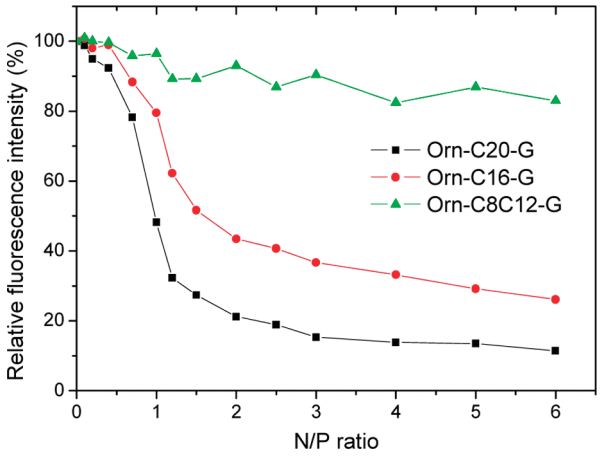

Figure 5. Exclusion of EtBr from CT-DNA complexes with bolas at different N/P ratios. The fluorescence intensity was normalized to 100% of the initial intensity.

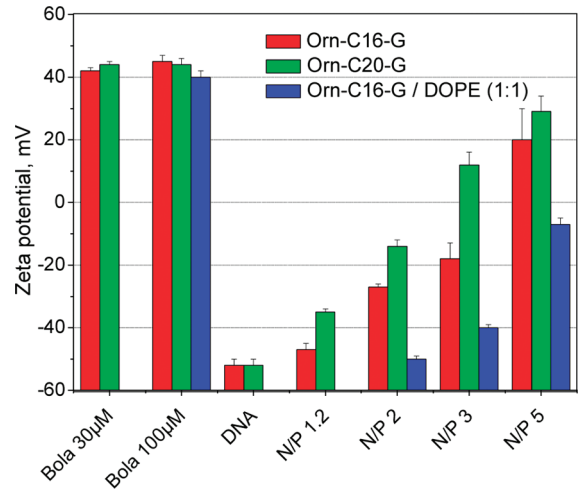

Figure 6. ζ-potential of nanostructures formed by bolas alone and by their formulations with DOPE and CT-DNA in MES buffer (pH 7.4) at different N/P ratios.

weak interaction with DNA. In contrast, both Orn-C16-G and Orn-C20-G showed a sharp decrease of EtBr fluorescence at N/P around 1. Thus, in accordance with the gel electrophoresis data it is confirmed that these bolas bind strongly to DNA by showing a significant level of DNA condensation. It can be also noticed that, similarly to the gel electrophoresis data, Orn-C20-G shows an EtBr fluorescence decrease at lower N/P ratio as compared to Orn-C16-G. Moreover, the fluorescence decrease is stronger for the former bola (ca. 85% for Orn-C20-G as compared to ca. 70% for Orn-C16-G). Thus, we can conclude that Orn-C20-G presents a stronger affinity to DNA and condense it more significantly as compared to Orn-C16-G. This conclusion corroborates with the observed stronger ability of Orn-C20-G to self-assemble without DNA evidenced by 1,8-ANS data. Since Orn-C8-C12-G shows a poor affinity to DNA and almost a negligible DNA condensation ability, we excluded this compound from further characterization, focusing only on Orn-C16-G and Orn-C20-G bolas.

Structural Characterization of Bolaplexes. To estimate the size of the obtained bolaplexes, DLS technique was used. Initially, the bolaplexes at different N/P ratios were prepared by direct addition of increasing quantities of Orn-C16-G from stock to pDNA solution. It was observed that at low N/P ratios, the particle size was relatively small (around 100 nm), while above N/P 1.2, their size increased rapidly reaching a maximum at N/P 2 (700 nm) and then further decreases until N/P 5 (see Supporting Information). In a second approach, the bolaplexes were prepared by mixing equal volumes of bolas and DNA aqueous solutions, followed by 30 min incubation at RT. This method gave similar DLS results for low N/P ratios (1.2 and 2): relatively small particles at N/P = 1.2 and much larger at N/P = 2 (Table 1). It is important to note that for Orn-C16-G at lower concentration the bolaplexes at N/P 2 (30 min incubation) showed much smaller sizes (150 nm). In contrast, after 5 min of incubation, Orn-C16-G/pDNA complexes presented similar small sizes (ca. 150 nm) for both low and high bola concentrations. Thus, the higher bola concentration probably favors aggregation of bolaplexes into larger particles. At N/P 5, this preparation method (with 30 min incubation) also gave relatively large particles as for N/P 2. The observed discrepancy between the two methods of preparation for N/P 5 is probably related to the incubation time, since in the first approach the measurements were done 5 min after each addition. The DLS data obtained with Orn-C20-G were similar to those with Orn-C16-G (Table 1), so that bolaplexes were small at N/P ratio 1.2, while their size increased significantly at higher N/P ratios. Moreover, for Orn-C16-G/DOPE mixture (1:1), a similar increase in the size of the bolaplexes was observed at higher N/P ratios (Table 1). The observation of larger complexes at higher N/Ps differs clearly from behavior of polyplexes and lipoplexes. Indeed, the latter at N/Ps close to 1 show relatively large complexes because of neutral charge of the complex, while at higher N/Ps they are much smaller because of their strong positive charge (*35*−*37*). Interestingly, our observations are in line with recent reports on other bolas featuring cationic group on one end and a neutral sugar residue on the other (*23, 24*). Therefore, we can suggest that the increase in size of bolaplexes at higher N/Ps could be a special feature of this type of bolas, which is probably because their bolaplexes do not become positively charged at higher N/Ps. This hypothesis was verified by measuring the zeta potential of bolaplexes (Figure 6). The bolas alone showed strongly positive ζ-potentials, while the bolaplexes at low N/P ratios were negatively charged and reached neutrality at N/P ratios around 3. At N/P 5, the observed ζ-potential was positive, however, we suspect that it could be due to excess of bola molecules that do not complex with DNA, thus contributing to apparent positive potential values. For Orn-C16-G/DOPE mixture (1:1), the ζ-potentials were systematically more negative, though a clear neutralization of the complexes was observed at N/P 5 (Figure 6). We expect that, as shown in Figure 1B, the positively charged part of bola interacts with DNA, while the neutral sugar residue is exposed at the bolaplex surface. This structure may favor neutrality of the bolaplex at higher N/Ps. Presence of DOPE does not change this tendency, but only shifts the complex neutralization to higher N/P ratios.

To access the nanoscopic architecture of bolaplexes, we performed atomic force microscopy (AFM) measurements in liquid (buffer) phase on a mica surface. An efficient absorption of the bolaplexes (N/P 2 or 1.2) at the mica surface was achieved only in the presence of magnesium cations. This indicates that the bolaplexes at the studied N/P ratios are negatively charged, so that Mg^{2+} ions act as a link between bolaplexes and the negatively charged mica surface. Orn-C16-G bolaplexes with pDNA formed relatively small and spherical structures (Figure 7A). The average height and width of the particles were 12 and 120 nm, respectively, which correspond to an average particle volume of about 1.7×10^5 nm^3 and an equivalent spherical particle diameter of 70 nm. This size is smaller than the one observed by DLS for N/P 2 (12 μM bola). Several reasons may explain this discrepancy. At first, the smaller size particles observed by AFM is based on a particle by particle data analysis, while DLS measures an average size with higher sensitivity to larger particles. Indeed, the DLS data based on particle number

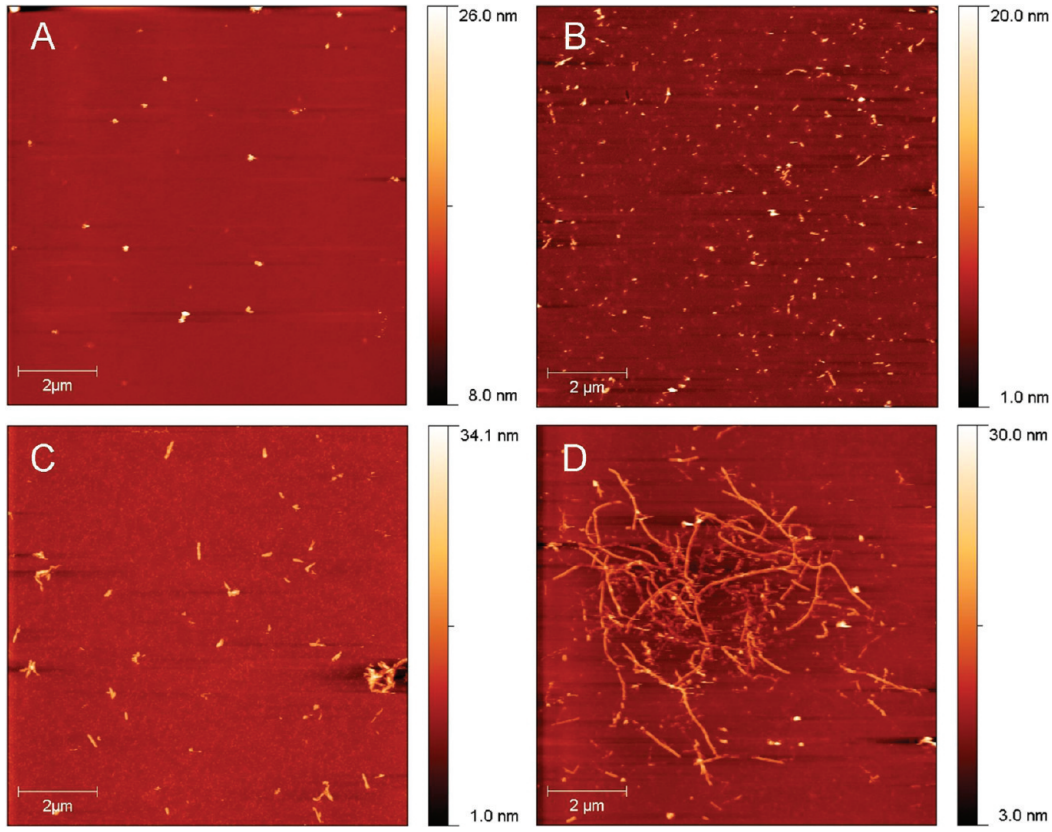

Figure 7. AFM images of Orn-C16-G (A and B, N/P 2) and Orn-C20-G (C and D, N/P 1.2) bolaplexes with pDNA (A and C) and CT-DNA (B and D). Images were obtained by tapping mode.

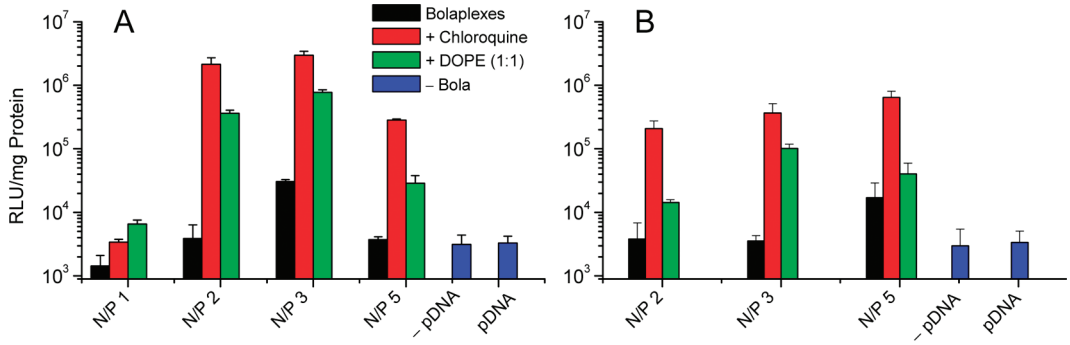

Figure 8. Transfection efficiency of the Orn-C16-G bolaplexes at different N/P ratios in COS-7 cells without (A) and with serum (B). Cells were incubated in serum-free Opti-MEM (A) or complete culture medium, DMEM containing 10% of FBS (B) with a bolaplex composed of plasmid DNA (1 μg per well), Orn-C16-G, and DOPE (when indicated). For some samples, the medium contained 100 μM chloroquine. After 3 h, 10% of FBS was added to the serum-free samples, while for all the samples with chloroquine the transfection medium was replaced with fresh complete culture medium. The luciferase activity quantification was performed after 48 h of incubation. Transfection efficiency determined from the luciferase assay was expressed as RLU/mg of protein. The negative controls were nontreated cells (-pDNA) and those transfected with naked pDNA (pDNA). The experiments were repeated six times for serum-free samples (A) and three times for samples with serum (B).

statistics is much closer to AFM data than those based on volume analysis (Table 1). Moreover, DLS data provides a hydrodynamic size of the particles, which is larger than the real size. Finally, in AFM measurements, the particles are stabilized by adsorption at the surface, while in DLS they are free in solution and can further aggregate to form larger particles. Bolaplexes of Orn-C16-G with CT-DNA showed high polydispersity and formed both spherical and short rodlike structures (Figure 7B). The presence of short rods of 8−10 nm height, 40−60 nm width, and 300−600 nm length could be explained by the linear structure of CT-DNA that favored the formation of elongated structures. In contrast, Orn-C20-G/DNA bolaplexes at N/P 2 were very large and polydisperse, in line with DLS data, which prompted us to study the bolaplexes at N/P 1.2. Remarkably, the complexes at N/P 1.2 showed predominantly rodlike structures for both pDNA and CT-DNA (Figure 7C and D). However, in the case of pDNA, the observed rods were relatively short, having height and width around 10 and 120 nm, respectively, while in the case of CT-DNA, they correspond to very long fibers of 16 nm height and 80 nm width. The formation of these "spaghetti-like" structures was previously reported for cationic lipids (*38*). It was proposed that in this kind of structure, the DNA molecule is located in the core, being surrounded by the lipid membrane. Probably, Orn-C20-G/CT-DNA bolaplexes present a similar structure, where single or multiple DNA strands are surrounded by a monolayer of bola molecules, similarly to the idealistic model in Figure 1B.

Transfection Efficiency and Cytotoxicity. The transfection efficiency of bolaplexes was in serum-free and serum-containing media for the different formulations by using the luciferase expression assay (Figure 8). For serum-free samples (Figure 8A), considerable transfection efficiency was observed for Orn-C16-G bolaplexes at N/P 2, 3, and 5 only in the presence of helper lipid DOPE or the endosomolytic reagent chloroquine (*28*). The better efficiency observed in the presence of DOPE is in line with previously reported data concerning other bolaamphiphiles (*21, 23*). DOPE probably improves the fusion of bolaplexes with cellular and endosomal membranes (*39, 40*). However, the strong effect of chloroquine on bolaplexes delivery is reported for the first time. This result clearly shows that the key barrier for internalization of bolaplexes is related to the endosomal escape. In the presence of serum, the transfection efficiency decreased significantly for all samples with DOPE (Figure 8B), which is in line with previous reports showing that DOPE-containing lipoplexes are highly sensitive to serum (*41*). In the presence of chloroquine, the effect of serum was less important, and the transfection efficiency increased systematically at higher N/P ratio. At N/P = 5, the sample with serum showed even slightly higher transfection efficiency than that without serum (Figure 8). Similar results were reported for lipoplexes, where higher N/Ps increased their resistance to serum (*42*).

On the other hand, bolaplexes of Orn-C20-G displayed relatively poor transfection efficiency for most of the formulations, which can be related to their larger size and spaghetti-like architecture (Figure 7). It should be noted that the observed values of transfection efficiency for Orn-C16-G were significantly lower than that for highly efficient commercial agent jetPEI (3×10^8 RLU/mg protein in the present study), while they were comparable with those recently reported for some other bolaamphiphiles (*21, 22*). Taking into account that the area of bolaamphiphiles as nonviral vectors is still poorly explored, we believe that there is a lot of room for improvement of their transfection efficiency. It will require optimization of bola chemical structure to achieve better control on the size and stability of the bolaplexes as well as on their ability to escape from endosomes. This work is currently in progress and will be reported in due course.

MTT-based assay suggested that new bolas do not show any considerable cytotoxicity. In the concentration range 30−200 μM of bolas with 48 h incubation, the observed cell viability was >80%, while for jetPEI (150 μM, expressed for nitrogen residues) it was only about 60% (see Supporting Information). The MTT results correlated well with the observed relatively high total protein (>80% vs. control) after 48 h of transfection with bolaplexes. This low cytotoxicity of the new bolas is an important advantage compared to polyplexes and lipoplexes. Thus, the obtained results showed the potentials of the new bolas molecules, especially Orn-C16-G, for the elaboration of highly efficient nonviral vectors.

CONCLUSIONS

We have synthesized three new bolaamphiphiles, bearing cationic and neutral groups at opposite sides of a hydrophobic spacer. The two bolaamphiphiles with more hydrophobic spacers exhibit low critical aggregation concentration and stronger affinities to DNA. At low N/P ratio (1.2), these bolas form bolaplexes of relatively small size, showing spherical and rodlike structures, while at higher N/P ratio their size increases due to neutralization of the complexes. Bolaplexes showed considerable transfection efficiency only in presence of the helper lipid DOPE or the endosomolytic agent chloroquine, indicating that the endosomal escape constitutes the main barrier to the internalization of these complexes. The present work provides strong basis for a further development of new efficient gene delivery vectors based on this original class of compounds.

ACKNOWLEDGMENT

This work was supported by Fondation pour la Recherche Médicale (FRM). We thank the groups of J.-S. Remy and B. Frisch for help with luminometry and DLS measurements. We also thank G. Zuber for fruitful discussions.

Supporting Information Available: Procedures for synthesis of Orn-C20-G and Orn-C8-C12-G. Some DLS data. Total protein and MTT-based cytotoxicity assays. This material is available free of charge via the Internet at http://pubs.acs.org.

LITERATURE CITED

(1) Fuhrhop, J. H., and Wang, T. (2004) Bolaamphiphiles. *Chem. Rev. 104*, 2901–2938.
(2) Damste, J. S. S., Schouten, S., Hopmans, E. C., Van Duin, A. C. T., and Geenevasen, J. A. J. (2002) Crenarchaeol: The characteristic core glycerol dibiphytanyl glycerol tetraether membrane lipid of cosmopolitan pelagic crenarchaeota. *J. Lipid Res. 43*, 1641–1651.
(3) Derosa, M., Gambacorta, A., and Gliozzi, A. (1986) Structure, Biosynthesis, And Physicochemical Properties Of Archaebacterial Lipids. *Microbiol. Rev. 50*, 70–80.
(4) Stetter, K. O. (1996) Hyperthermophilic procaryotes. *FEMS Microbiol. Rev. 18*, 149–158.
(5) Shimizu, T., Masuda, M., and Minamikawa, H. (2005) Supramolecular nanotube architectures based on amphiphilic molecules. *Chem. Rev. 105*, 1401–1443.
(6) Kameta, N., Masuda, M., Minamikawa, H., Mishima, Y., Yamashita, I., and Shimizu, T. (2007) Functionalizable organic nanochannels based on lipid nanotubes: Encapsulation and nanofluidic behavior of biomacromolecules. *Chem. Mater. 19*, 3553–3560.
(7) Wang, X., and Liang, Y. (2001) Formation of monolayer lipid membranes in water and ethanol from bolaamphiphiles. *J. Colloid Interface Sci. 233*, 364–366.
(8) Mintzer, M. A., and Simanek, E. E. (2009) Nonviral vectors for gene delivery. *Chem. Rev. 109*, 259–302.
(9) Martin, B., Sainlos, M., Aissaoui, A., Oudrhiri, N., Hauchecorne, M., Vigneron, J. P., Lehn, J. M., and Lehn, P. (2005) The design of cationic lipids for gene delivery. *Curr. Pharm. Des. 11*, 375–394.
(10) Safinya, C. R. (2001) Structures of lipid-DNA complexes: Supramolecular assembly and gene delivery. *Curr. Opin. Struct. Biol. 11*, 440–448.
(11) Chesnoy, S., and Huang, L. (2000) Structure and function of lipid-DNA complexes for gene delivery. *Annu. Rev. Biophys. Biomol. Struct. 29*, 27–47.
(12) Hirko, A., Tang, F., and Hughes, J. A. (2003) Cationic lipid vectors for plasmid DNA delivery. *Curr. Med. Chem. 10*, 1185–1193.
(13) Huang, L., Hung, M.-C., and Wagner, E., Eds. (1999) *Nonviral Vectors for Gene Therapy*, Academic Press, London.
(14) Demeneix, B., Hassani, Z., and Behr, J. P. (2004) Towards multifunctional synthetic vectors. *Curr. Gene. Ther. 4*, 445–455.
(15) Mastrobattista, E., van der Aa, M. A. E. M., Hennink, W. E., and Crommelin, D. J. A. (2006) Artificial viruses: a nanotechnological approach to gene delivery. *Nat. Rev. Drug Discovery 5*, 115–121.
(16) Nishikawa, M., and Huang, L. (2001) Nonviral vectors in the new millennium: Delivery barriers in gene transfer. *Hum. Gene Ther. 12*, 861–870.
(17) Zuber, G., Dauty, E., Nothisen, M., Belguise, P., and Behr, J. P. (2001) Towards synthetic viruses. *Adv. Drug Delivery Rev. 52*, 245–253.
(18) Zuber, G., Zammut-Italiano, L., Dauty, E., and Behr, J. P. (2003) Targeted gene delivery to cancer cells: Directed assembly

of nanometric DNA particles coated with folic acid. *Angew. Chem., Int. Ed. 42*, 2666–2669.
(19) Zhang, S., Zhao, Y., Zhao, B., and Wang, B. (2010) Hybrids of Nonviral Vectors for Gene Delivery. *Bioconjugate Chem. 21*, 1003–1009.
(20) Koltover, I., Salditt, T., Radler, J. O., and Safinya, C. R. (1998) An inverted hexagonal phase of cationic liposome-DNA complexes related to DNA release and delivery. *Science 281*, 78–81.
(21) Gaucheron, J., Santaella, C., and Vierling, P. (2001) In vitro gene transfer with a novel galactosylated spermine bolaamphiphile. *Bioconjugate Chem. 12*, 569–575.
(22) Fabio, K., Gaucheron, J., Di Giorgio, C., and Vierling, P. (2003) Novel galactosylated polyamine bolaamphiphiles for gene delivery. *Bioconjugate Chem. 14*, 358–367.
(23) Brunelle, M., Polidori, A., Denoyelle, S., Fabiano, A. S., Vuillaume, P. Y., Laurent-Lewandowski, S., and Pucci, B. (2009) A structure-activity investigation of hemifluorinated bifunctional bolaamphiphiles designed for gene delivery. *C. R. Chim. 12*, 188–208.
(24) Denoyelle, S., Polidori, A., Brunelle, M., Vuillaume, P. Y., Laurent, S., ElAzhary, Y., and Pucci, B. (2006) Synthesis and preliminary biological studies of hemifluorinated bifunctional bolaamphiphiles designed for gene delivery. *New J. Chem. 30*, 629–646.
(25) Eaton, M. A. W., Baker, T. S., Catterall, C. F., Crook, K., Macaulay, G. S., Mason, B., Norman, T. J., Parker, D., Perry, J. J. B., Taylor, R. J., Turner, A., and Weir, A. N. (2000) A new self-assembling system for targeted gene delivery. *Angew. Chem., Int. Ed. 39*, 4063–4067.
(26) Réthoré, G., Montier, T., Le Gall, T., Delépine, P., Cammas-Marion, S., Lemiègre, L., Lehn, P., and Benvegnu, T. (2007) Archaeosomes based on synthetic tetraether-like lipids as novel versatile gene delivery systems. *Chem. Commun. 20*, 2054–2056.
(27) Lainé, C., Mornet, E., Lemiègre, L., Montier, T., Cammas-Marion, S., Neveu, C., Carmoy, N., Lehn, P., and Benvegnu, T. (2008) Folate-equipped pegylated archaeal lipid derivatives: Synthesis and transfection properties. *Chem.—Eur. J. 14*, 8330–8340.
(28) Cotten, M., Langle-Rouault, F., Kirlappos, H., Wagner, E., Mechtler, K., Zenke, M., Beug, H., and Birnstiel, M. L. (1990) Transferrin-polycation-mediated introduction of DNA into human leukemic cells: Stimulation by agents that affect the survival of transfected DNA or modulate transferrin receptor levels. *Proc. Natl. Acad. Sci. U.S.A. 87*, 4033–4037.
(29) Mosmann, T. (1983) Rapid colorimetric assay for cellular growth and survival: Application to proliferation and cytotoxicity assays. *J. Immunol. Meth. 65*, 55–63.
(30) Slavik, J. (1982) Anilinonaphthalene Sulfonate as a Probe of Membrane-Composition and Function. *Biochim. Biophys. Acta 694*, 1–25.
(31) Lentz, B. R. (1993) Use of fluorescent probes to monitor molecular order and motions within liposome bilayers. *Chem. Phys. Lipids 64*, 99.
(32) M'Baye, G., Mely, Y., Duportail, G., and Klymchenko, A. S. (2008) Liquid ordered and gel phases of lipid bilayers: fluorescent probes reveal close fluidity but different hydration. *Biophys. J. 95*, 1217–1225.
(33) Meister, A., and Blume, A. (2007) Self-assembly of bipolar amphiphiles. *Curr. Opin. Colloid Interface Sci. 12*, 138–147.
(34) Lleres, D., Dauty, E., Behr, J. P., Mely, Y., and Duportail, G. (2001) DNA condensation by an oxidizable cationic detergent. Interactions with lipid vesicles. *Chem. Phys. Lipids 111*, 59–71.
(35) Pitard, B., Oudrhiri, N., Vigneron, J. P., Hauchecorne, M., Aguerre, O., Toury, R., Airiau, M., Ramasawmy, R., Scherman, D., Crouzet, J., Lehn, J. M., and Lehn, P. (1999) Structural characteristics of supramolecular assemblies formed by guanidinium-cholesterol reagents for gene transfection. *Proc. Natl. Acad. Sci. U.S.A. 96*, 2621–2626.
(36) Xu, Y., Hui, S. W., Frederik, P., and Szoka, F. C., Jr. (1999) Physicochemical characterization and purification of cationic lipoplexes. *Biophys. J. 77*, 341–353.
(37) Findeis, M. A., Ed. (2001) *Nonviral Vectors for Gene Therapy: Methods and Protocols*, Humana Press, Clifton, NJ.
(38) Sternberg, B., Sorgi, F. L., and Huang, L. (1994) New structures in complex formation between DNA and cationic liposomes visualized by freeze-fracture electron microscopy. *FEBS Lett. 356*, 361–366.
(39) Felgner, J. H., Kumar, R., Sridhar, C. N., Wheeler, C. J., Tsai, Y. J., Border, R., Ramsey, P., Martin, M., and Felgner, P. L. (1994) Enhanced gene delivery and mechanism studies with a novel series of cationic lipid formulations. *J. Biol. Chem. 269*, 2550–2561.
(40) Farhood, H., Serbina, N., and Huang, L. (1995) The role of dioleoyl phosphatidylethanolamine in cationic liposome mediated gene transfer. *Biochim. Biophys. Acta 1235*, 289–295.
(41) Li, S., Tseng, W. C., Beer Stolz, D., Wu, S. P., Watkins, S. C., and Huang, L. (1999) Dynamic changes in the characteristics of cationic lipidic vectors after exposure to mouse serum: Implications for intravenous lipofection. *Gene Ther. 6*, 585–594.
(42) Yang, J. P., and Huang, L. (1997) Overcoming the inhibitory effect of serum on lipofection by increasing the charge ratio of cationic liposome to DNA. *Gene Ther. 4*, 950–960.

BC100334T